FULL PAPER

Linear Dendritic Block Copolymers as Promising Biomaterials for the Manufacturing of Soft Tissue Adhesive Patches Using Visible Light Initiated Thiol–Ene Coupling Chemistry

*Viktor Granskog, Oliver C. J. Andrén, Yanling Cai, Marcela González-Granillo, Li Felländer-Tsai, Hans von Holst, Lars-Arne Haldosen, and Michael Malkoch**

A library of dendritic–linear–dendritic (DLD) materials comprising linear poly(ethylene glycol) and hyperbranched dendritic blocks based on 2,2-bis(hydroxymethyl) propionic acid is successfully synthesized and post-functionalized with peripheral allyl groups. Reactive DLDs with pseudo-generations of 3 to 6 (G3-G6) are isolated in large scale allowing their thorough evaluation as important components for the development of biomedical adhesives. Due to their branched nature and inherent degradable ester-bonds, promising biomaterial resins are accomplished with suitable viscosity, eliminating the excessive use of co-solvents. By utilizing benign high-energy visible light initiated thiol–ene coupling chemistry, DLDs together with tris[2-(3-mercaptopropionyloxy)ethyl] isocyanurate and surgical mesh enable the fabrication of soft tissue adhesive patches (STAPs) within a total irradiation time of 30 s. The STAPs display the ability to create good adhesion to wet soft tissue and encouraging results in cytotoxicity tests. All crosslinked materials are also found to degrade after being stored in human blood plasma and phosphate buffered saline. The proposed benign methodology coupled with the promising features of the crosslinked materials is herein envisioned as a soft tissue adhesive with properties that do not exist in currently available tissue adhesives.

1. Introduction

The use of adhesive sealants and glues in biomedical applications has increased the freedom for surgeons by providing more enhanced treatment options considering function and comfort for the patients but also in economic aspects.[1] There is a variety of commercially available biomedical tissue adhesives, both based on natural and synthetic components, with varying properties, e.g., adhesion, elastic modulus, and biocompatibility.[2,3] In this context, it is apparent that current adhesives have not reached their full potential, partially prevented by either inadequate bond strength or doubtful biocompatibility of the adhesive materials.[4,5] Still, the interest in surgical adhesives is growing.[6] For instance, fixation of the steadying mesh with natural fibrin glue in hernia repairs has displayed promising results as an emerging new technique that complements tackers and staples.[7] Independent of being natural or synthetic methods, the great possibilities encourage researchers to continue their quest in proposing novel material concepts that aim to fulfill the criteria set for today's nonexisting adhesives.

From the countless numbers of material concepts with potential use as biomedical adhesives, functional dendritic polymers belong to the most intriguing. These highly branched and reactive polymers are typically exploited as scaffolds in drug delivery systems and tissue engineering.[8] Their large number of functional groups located at the outer layer of the polymer are perfectly suited for network formation. This was exploited by Grinstaff and co-workers allowing monodisperse poly(glycerol-succinic acid) dendrimers to be used in the field of ophthalmic surgery.[9,10] While monodisperse dendrimers are perfect test beds for the understanding of structure-to-property relationships, their synthetic realization makes them less attractive, especially from a large-scale production and availability point of view. A promising alternative is based on their less perfect analog, i.e., hyperbranched polymers. Hyperbranched

V. Granskog, O. C. J. Andrén, Dr. Y. Cai, Prof. M. Malkoch
Department of Fibre and Polymer Technology
KTH Royal Institute of Technology
SE-100 44 Stockholm, Sweden
E-mail: malkoch@kth.se
Dr. M. González-Granillo, Prof. L. Felländer-Tsai
Department of Clinical Science Intervention and Technology
Karolinska Institutet
SE-141 86 Stockholm, Sweden
Prof. H. von Holst
Division of Neuronic Engineering
KTH Royal Institute of Technology
SE-141 52 Huddinge, Sweden
Prof. L.-A. Haldosen
Department of Biosciences and Nutrition
Karolinska Institutet
SE-141 83 Huddinge, Sweden

DOI: 10.1002/adfm.201503235

polymers have a typical degree of branching (DB) between 0.4 and 0.8 compared to dendrimers with a DB of 1.[11] While being less perfect than dendrimers, the obtained properties of hyperbranched polymers are similar to dendrimers. From a commercialization point of view, the pseudo one-pot synthesis enables large-scale production of these polymers making them ideal candidates as biomedical adhesives.[12] For instance, a new hyperbranched polymer based on a mussel-inspired structure has displayed encouraging properties for use as biomedical adhesives.[13,14] The structural features of dendritic polymers give rise to beneficial physical and chemical properties well-suited for components in biomedical adhesives. The highly branched architecture prevents chain entanglement leading to a molecular movement presumed to be more of a translational character instead of the segmental movement considered for linear polymers.[15] Importantly, dendritic polymers offer a molecular weight of one order of magnitude higher compared to their linear analog with the same viscosity.[16] As a result, high molecular weight dendritic resins with suitable viscosities can be exploited without introducing a solvent. The use of solvent-free resins based on highly functional polymers instead of smaller functional molecules reduces the leakage of unreacted components to surrounding tissue with increased biocompatibility as a consequence. This can be compared to the typically used resins today in high-performance adhesives like dental adhesives and cyanoacrylates. With respect to adhesive components, the large amount of peripheral end-group representation enables the formation of multifunctional dendritic crosslinking sites. One of the many efficient reactions, UV light initiated thiol–ene coupling (TEC) chemistry is of high interest for achieving biocompatible adhesives for surgical purposes. TEC is recognized as a benign and efficient reaction being insensitive to oxygen.[17] The latter is of great importance as operations are typically executed in surgical environments. The favorable properties of TEC in adhesives also include a gelation point at high conversions due to a stepwise network formation of flexible thioether linkages. The high gelation point reduces the curing induced shrinkage and increases the final conversion of the crosslinked network.[17] High final conversion of functional groups has even been presented for hyperbranched polymers despite high molecular weight and multifunctionality using TEC chemistry.[18]

In this study, we propose a novel family of biomedical patches based on dendritic–linear–dendritic (DLD) hybrids and their adhesive ability toward soft tissue porcine skin in the form of soft tissue adhesive patches (STAPs) as a model system for the evaluation of various internal wound repairs, a method originated from the earlier developed Fiber Reinforced Adhesive Patch technology.[19] Compared to existing tissue adhesives, this system aims for not only good adhesion but also sufficient mechanical integrity for mesh fixation. The methodology goes beyond UV light initiations and capitalizes on high-energy visible (HEV) light initiated TEC chemistry, where allyl-activated DLD hybrids that together with a clinically used surgical mesh and a trithiol component transform to adhesive patches under benign and wet conditions. The patches were compared to patches with the commercial tissue adhesive Histoacryl based on 2-butyl cyanoacrylate, known for its high tissue adhesion but lacking the biocompatibility needed for legitimate internal use.[3,5,20]

2. Results and Discussion

2.1. Library of DLD Hybrids

The use of dendritic macromolecules as biomedical adhesives has shown promising results due to the multiple representations of available end groups that can efficiently create highly crosslinked networks. Such a large number of available sites can also be exploited for the introduction of additional therapeutic function to the adhesive.[9,13,21] In this case, to facilitate the use of dendritic polymers with large-scale prerequisites, i.e., for biomedical adhesives, hyperbranched polymers are the natural substitute to the more synthetically demanding and monodisperse dendrimers. Consequently, DLD hybrids consisting of a hydrophilic 2 kDa poly(ethylene glycol) (PEG) core and hydrophobic hyperbranched structures based on 2,2-bis(hydroxymethyl) propionic acid (bis-MPA) with allyl-functional end-groups were synthesized and evaluated for their potential use as biomedical adhesive components. The building blocks were carefully chosen with respect to their biocompatibility along with biodegradable profile of the dendritic segments.[22] The procedure used to synthesize the DLDs was straightforward and resulted in hyperbranched structures of intentional dendritic sizes.[12] Four different DLDs of pseudo-generations of 3 to 6 (G3-G6) displaying 16 to 128 reactive allyl groups were synthesized on a 40 g scale to systematically assess the structure-to-property relationships of the materials. Tris[2-(3-mercaptopropionyloxy)ethyl] isocyanurate (TEMPIC) was chosen as a complementary tri-thiol crosslinking component for photoinitiated TEC chemistry. The choice of using TEMPIC was based on its excellent miscibility with the DLDs along with previously shown encouraging results as a component for biomedical adhesives, both in terms of adhesion and cytotoxicity.[23]

To fully understand their potential in a biomedical adhesive, the DLDs were examined both as single compounds as well as components in crosslinked adhesives (**Scheme 1**). NMR and size exclusion chromatography (SEC) analyses detail an expected increase in number average molecular weight (M_n) with increasing pseudo-generation. The deviating values of M_n from SEC data, compared to NMR and theoretical (theo.) calculations (**Table 1**), can be explained by poor correlation between the calibration with linear polymers and the analyzed hybrids. Dispersities of 1.03–1.74 were obtained with a predictable increase for higher pseudo-generations due to the irregular nature of hyperbranched block. The DB for the DLDs was obtained using the Frechet equation, Formula 1,[24] combined with collected data from quantitative ^{13}C-NMR spectrum of the DLDs scaffolds prior to allylation reactions. Consistent with earlier reported results, the DB for DLDs ranges from 0.43 to 0.53.[12,25]

Thermal analyses using differential scanning calorimetry (DSC) show crystallinity for allylated DLD-G3 and DLD-G4 with melting temperatures (T_m) of 30 and 22 °C, respectively. These values are lower than the T_m of the corresponding allylated 2 kDa PEG detected at 42 °C. The higher pseudo-generations, i.e., DLD-G5 and DLD-G6, did not exhibit any crystalline behavior. Furthermore, the glass-transition temperatures (T_g) increased from −54 to −44 °C with increasing the pseudo-generation from G3 to G6.

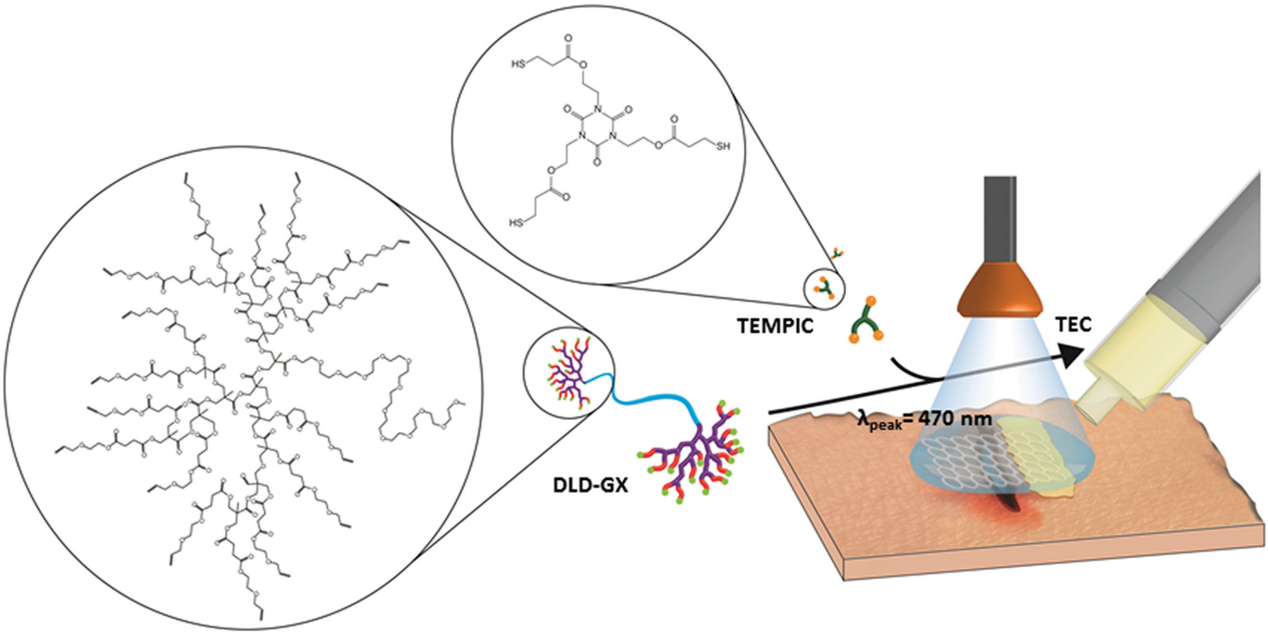

Scheme 1. Schematic representation of potential usage of DLD-G*X* crosslinked with TEMPIC (DLD-G*X* × TEMPIC) patches. The soft tissue adhesive patch is easily applied and gently cured through TEC upon light initiation with HEV-light in order to stabilize a soft tissue wound.

The low glass-transition temperature and the reduction of crystallinity due to the dendritic blocks lead to viscous liquids and allowed their use as neat adhesive components without the introduction of a co-solvent.

Rheological measurements were then performed to understand the relationship between the pseudo-generations and final viscosity of the polymers. The crystalline DLD-G3 was found to have the highest viscosity and exhibited shear thinning behavior at 25 °C (**Figure 1**). This is in direct contrast to the DLD components of higher generations which were found to exhibit Newtonian behavior with the viscosity highly dependent on the size of the hyperbranched structures. In this case, DLD-G6 noted the highest viscosity of 75 Pa s, followed by DLD-G5 and DLD-4 with viscosities of 30 and 17 Pa s, respectively. Unlike melts of linear polymers that usually display shear thinning behavior, the DLD melts show Newtonian behavior that follow earlier demonstrated melt properties of hyperbranched polymers and dendrimers.[26] In order to circumvent the crystallization of DLD-G3 and enable a fair comparison between the different DLDs, the rheological properties were also investigated at 35 °C. All components showed a decrease in their viscosity at 35 °C with DLD-G6 displaying the highest viscosity of 21 Pa s followed by a decreasing viscosity with decreasing pseudo-generation to 12 and 7 Pa s for DLD-G5 and DLD-G4, respectively, exhibiting Newtonian behavior. Interestingly, the DLD-G3 in its melted state revealed the lowest viscosity of 3 Pa s and changed its rheological behavior from shear thinning to Newtonian. These rheological properties are important features for appropriate application of adhesives on soft tissue prior to crosslinking to generate STAPs.

2.2. Network Formation Based on DLD Hybrids

In the context of chemically crosslinking the resins, a curing lamp intended for light-cured dental materials (Bluephase 20i) was used. By employing Bluephase 20i that emits light with a dominant wavelength of 470 nm with the intensity of 1200 mW cm^{-2}, the concerns of tissue damage from traditional UV-irradiation are reduced. Together with the mild and robust reaction of TEC chemistry, the use of higher wavelengths was found to provide a gentle curing procedure that

Table 1. Material characteristics of the analyzed allylated DLD hybrids. Thermal properties, molecular weight, dispersity, degree of branching, and number of functional end groups for each DLD are shown.

Polymers	T_g [°C]	T_m [°C]	M [g mol^{-1}] (theo.)	M_n [g mol^{-1}] (NMR)	M_n [g mol^{-1}] (SEC)	$Đ$	DB	No. of functional end groups (theo.)	No. of functional end groups (NMR)
DLD-G3	–54	30	6334	5595	3000	1.06	0.53	16	13
DLD-G4	–49	22	11442	11092	3200	1.33	0.48	32	31
DLD-G5	–47	x	21116	20705	3800	1.52	0.42	64	62
DLD-G6	–43	x	40465	40476	4500	1.74	0.43	128	128

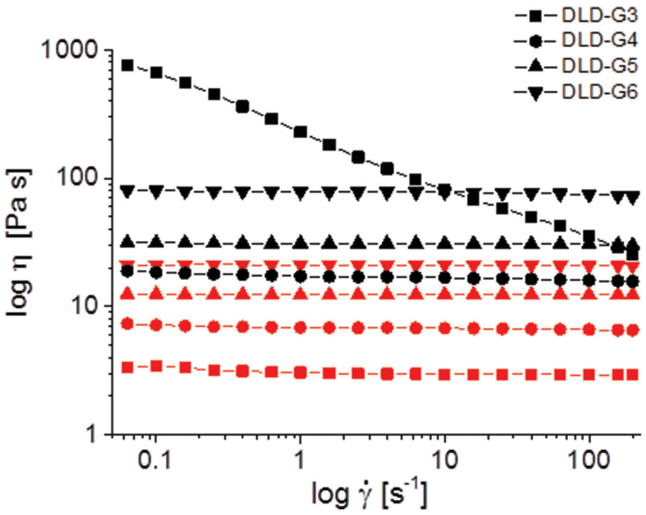

Figure 1. Results from viscosity measurements of the DLDs at varying shear rates display the different viscosities and rheological behavior of the DLD components at 25 °C (black) and 35 °C (red).

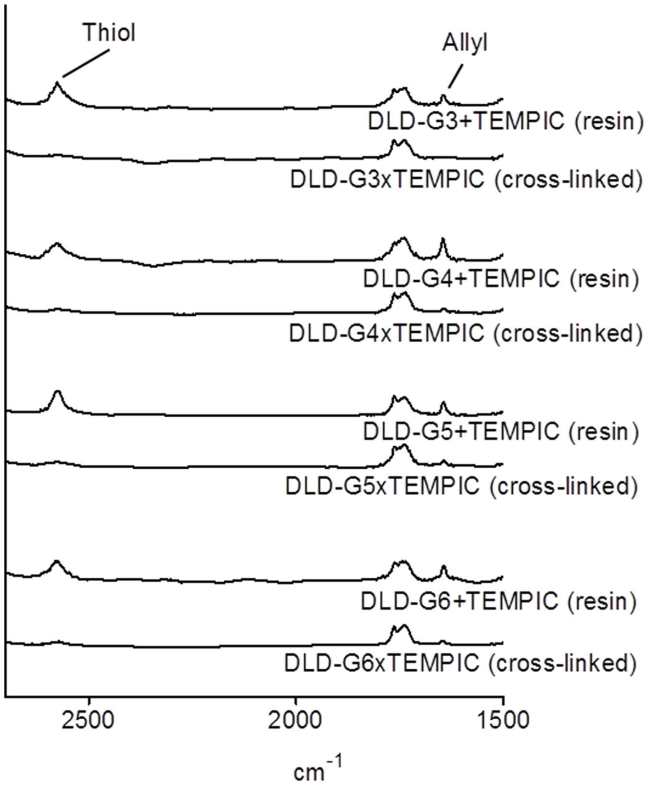

Figure 2. FT-Raman spectra from measurements on both resins and crosslinked materials of the DLDs mixed with TEMPIC. The crosslinked materials were cured with 30 s of irradiation using Bluephase 20i and a high conversion of functional groups is displayed.

without doubt could be established during minimally invasive surgery. This was confirmed by Fourier transform Raman (FT-Raman) spectroscopy of the formation of crosslinked materials upon light irradiation for only 30 s. High conversions of thiol (2575 cm^{-1}) and allyl (1645 cm^{-1}) groups can be seen by comparing the spectra of the resins after network formation (**Figure 2**). The conversion of functional groups was similar for all DLD hybrids. In order to obtain the gel fractions (GFs) (Table S1, Supporting information), the crosslinked networks were leached in chloroform. The observed GFs of DLD-G*X* crosslinked with TEMPIC (DLD-G*X* × TEMPIC) were above 90% for DLD-G4 × TEMPIC, DLD-G5 × TEMPIC, and DLD-G6 × TEMPIC while DLD-G3 × TEMPIC gave a lower value of 85.6%. Longer irradiation times did not demonstrate a significant increase in GF. Fascinatingly, the resins could also be cured without external stimuli or the addition of photoinitiator. This phenomenon was found for the higher pseudo-generations DLD-G5 and DLD-G6 in which the mixed resins started to gel spontaneously after only a few minutes. Fast spontaneous gelation of viscous liquids without external stimuli of initiation and from polymeric components is an interesting aspect for biomedical adhesives. These mechanisms may display an advantage over small molecule resins in which the large hyperbranched macromolecules with sterical structure are envisioned to have a lower tendency to penetrate healthy tissue and should therefore be studied further.

Swelling studies on the networks were performed in phosphate buffered saline (PBS) with a pH of 7.4 at a temperature of 37 °C to mimic physiological environment. The degree of swelling was measured at several time points (**Figure 3**a). The prepared networks were found to swell the most during the first day and generally reached equilibrium after 1 week. With increasing generation of the dendritic block, the materials exhibited a decrease in swelling with a minimum value of 13% for DLD-G5 × TEMPIC. However, the material with DLD-G5 displayed a lower swelling than the sample that contained DLD-G6, despite smaller hydrophobic hyperbranched blocks and half the amount of end groups for potential crosslinks per DLD molecule. This could be an effect of increased intramolecular cyclization where the conversion of functional groups does not contribute to an increased crosslinking density in the final network. The relatively low water uptake of the crosslinked materials shows an exceptional potential of the DLDs to provide PEG-based gels without their characteristic high water swelling properties.[27] A low swelling degree is of significant interest since swelling of implanted materials may cause pain and discomfort to the patient as well as promote adhesive failure. The apparent drawback of high swelling adhesives has recently also been highlighted by Messersmith and co-workers, who exploited block copolymers of PEG and poly(propylene oxide) to circumvent these issues.[28]

Mechanical properties of the crosslinked materials in their dry state and after storage in PBS or human blood plasma (HBP) at 37 °C were analyzed by tensile testing. As dry networks, the different sizes of the hyperbranched structures did not significantly alter the Young's modulus or maximum stress endurance (Figure 3b,c). Interestingly, for samples stored for 1 week in PBS, the Young's modulus was significantly increased with swelling for the materials with components of higher pseudo-generations than G3. The Young's modulus of the swollen gels ranged from 6.8 to 11.6 MPa with DLD-G6 × TEMPIC displaying the largest increase of 2.2-fold, from 5.2 to 11.6 MPa. Additionally, the maximum stress endurance also increased for the submerged networks reaching a maximum within 1 week for DLD-G5 × TEMPIC (1.1 MPa) and DLD-G6 ×

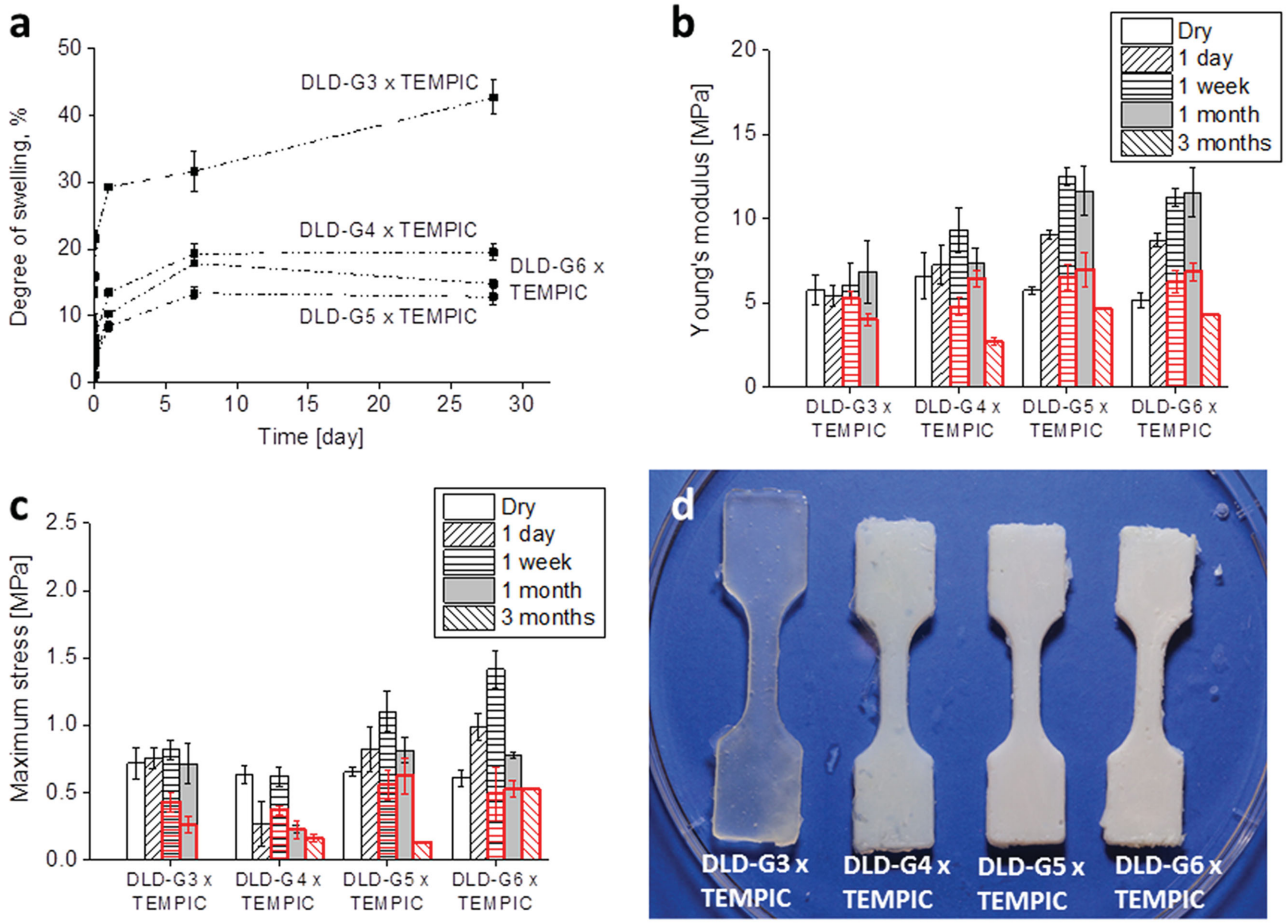

Figure 3. Material behavior of the DLDs crosslinked with TEMPIC. a) Swelling in PBS. b) Young's modulus in dry state and after storage in PBS (black) or in HBP (red). c) Maximum stress in dry state and after storage in PBS (black) or HBP (red). d) Appearance of the crosslinked materials after storage in PBS for 1 week.

TEMPIC (1.4 MPa). The networks based on DLD-G3 did not exhibit any significant changes in mechanical properties. From a visual observation after 1 week swelling in PBS, the networks based on DLD-G3 retained their translucent appearance while gels based on DLD-G4, -G5, and -G6 transitioned from being translucent to white in color, indicating a collapse of the hydrophobic hyperbranched structures (Figure 3d). Such a collapse, where the hydrophobic dendritic junction areas become more compact, is envisioned to generate stiffening properties of the crosslinked materials. All of the crosslinked materials except DLD-G3 × TEMPIC displayed indications of degradation with either decreased Young's modulus or maximum stress endurance or both after being stored in PBS for 1 month.

In contrast to PBS storage, the mechanical properties of the networks submerged in HBP did not follow the same behavior. The increase of Young's modulus and maximum stress endurance for the crosslinked networks with higher dendritic generations appeared to be delayed and the decrease in mechanical properties noted after 1 month of storage in PBS were unable to be determined for the study in HBP. However, all networks displayed significant deterioration of mechanical stability after 3 months in HBP with DLD-G3 × TEMPIC completely losing its structural integrity for tensile evaluation. The differences in mechanical properties compared to the study in PBS may be due to combination of different swelling equilibrium and faster degradation.

The weight loss of the materials stored in PBS and HBP (**Figure 4**) did not exceed the loss of material from the GF study and therefore cannot be correlated to degradation mechanisms. These results indicate bulk degradation of the crosslinked materials, where DLD-G4 × TEMPIC is the only network that decreased in strength after 1 month in both PBS and HBP but still maintained its mechanical integrity unlike DLD-G3 × TEMPIC after 3 months in HBP. It is apparent that the degree of swelling and the mechanical properties such as Young's modulus, stress endurance, and their sensitivity toward degradation in physiological conditions can straightforwardly be tuned by altering the size of the hyperbranched structure. Unfortunately, direct comparison to Histoacryl could not be performed due to poor bulk formation of the cyanoacrylate adhesive.

2.3. Adhesive Patch

Satisfied with the obtained properties of the networks based on DLD hybrids, a novel patch methodology was sought out for the biomedical adhesives. In contrast to traditional tissue gluing

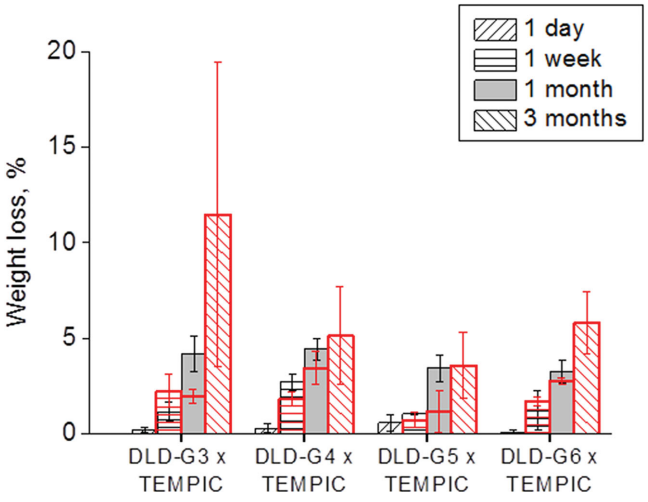

Figure 4. The weight loss of the DLDs crosslinked with TEMPIC after storage in PBS (black) or HBP (red).

adhesives, the DLD adhesives were used together with a surgical mesh to form a topological STAP that properly fixates wet porcine skin models (**Figure 5**a). The damaged tissue can either be covered by the adhesive as a patch or only fixed at the ends to allow penetration of body fluids (Figure 5b). For the adhesion tests, patches were cured with 1 min of irradiation using Bluephase 20i onto soaked porcine skin and then directly submerged in PBS and stored for 1 h at 37 °C. As a direct comparison, commercial tissue adhesive Histoacryl was applied using a similar strategy, excluding the light curing step. The bond shear strength was assessed (Figure 5c). Patches of DLD-G4 × TEMPIC provided significant adhesive strength of 21 kPa ($p < 0.05$ to the others) toward wet porcine skin, while patches of DLD-G5 × TEMPIC and DLD-G6 × TEMPIC gave strengths of 9.7 and 9.1 kPa, respectively. The adhesive prepared with DLD-G3 was not able to form a continuous thin film and was partly dissolved during storage in PBS but displayed an average value of 3.7 kPa. Histoacryl proved itself as the adhesive with the highest adhesive strength with 31 kPa ($p < 0.05$ to the others), of which the samples mainly failed cohesively in the top layer of the porcine skin. The patches containing DLD-G4, -G5, or -G6 failed adhesively at the adhesive–skin interface. Histoacryl and the dendritic networks, except DLD-G3 × TEMPIC, showed sufficient mechanical support and compatibility to the surgical mesh to endure the load applied. Importantly, the DLD-G4 × TEMPIC demonstrated the most promising results of the crosslinked DLD materials as a matrix for STAP with high adhesive ability to the difficult surface of wet porcine skin

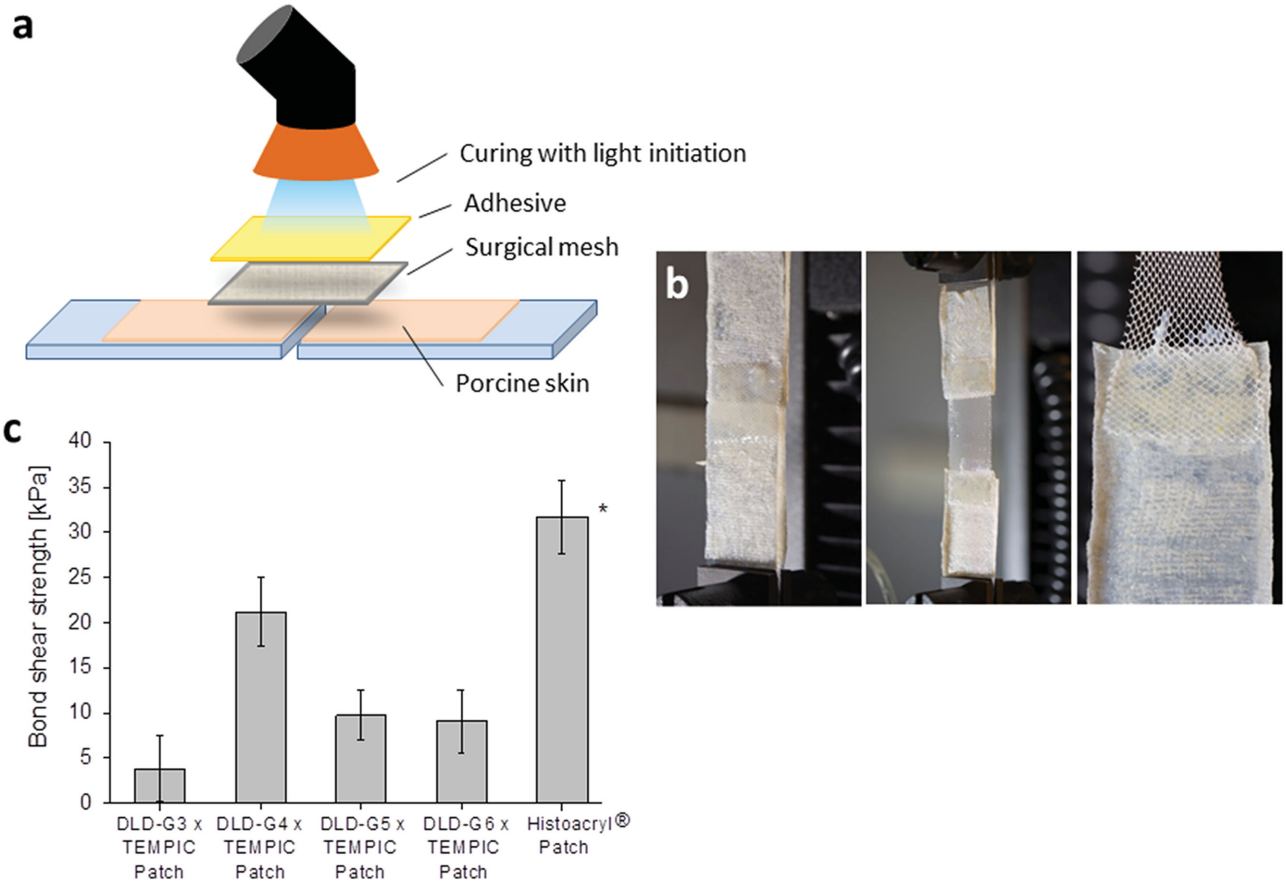

Figure 5. Adhesion test. a) Schematic image of preparation of test specimens. No light curing was used for Histoacryl. b) Test specimen of porcine skin glued together with a DLD-G4 × TEMPIC patch and an alternative fixation of the surgical mesh. c) Bond shear strength of the adhesive patches to wet porcine skin. *Cohesive failure in porcine skin.

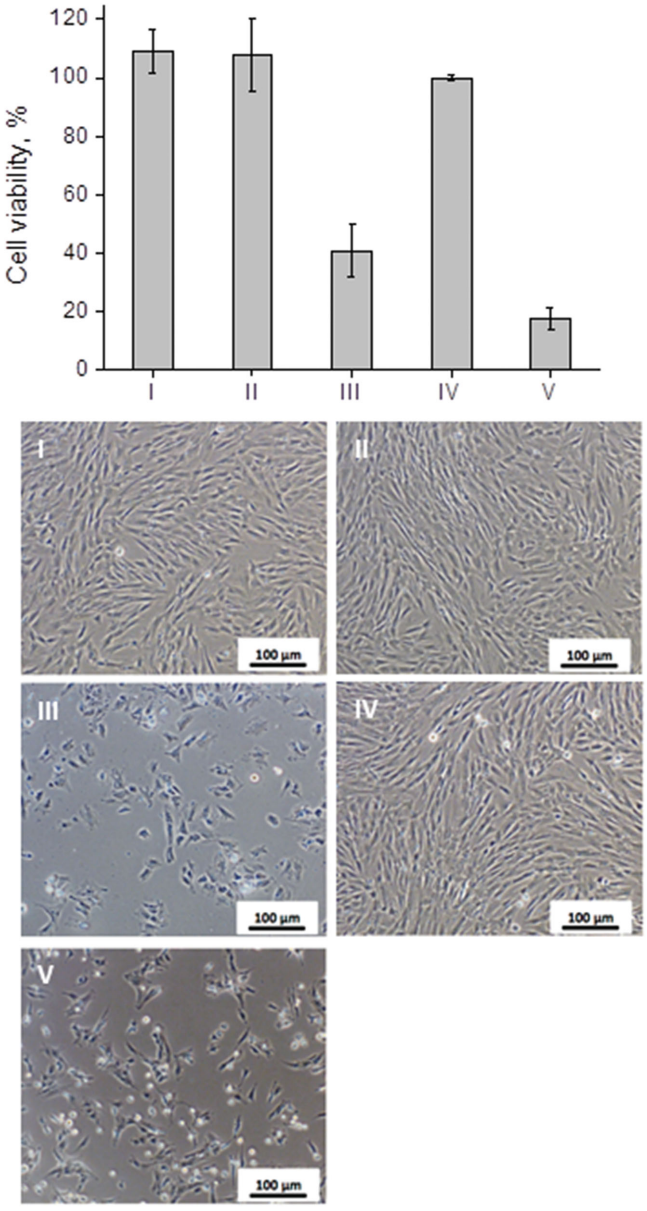

Figure 6. Cell viability of hDF cultured in CGM extracts of I) DLD-G4 × TEMPIC (no CQ), II) DLD-G4 × TEMPIC (0.1 wt% CQ), III) Histoacryl, IV) negative control, and V) positive control, with corresponding images displaying cell density and morphology.

with bond strengths that are close to the limit that the porcine skin as substrate could endure.

2.4. Cytotoxicity of Cured Materials

With respect to the envisioned application of the dendritic adhesives, two different test methods were sought out to probe the cytotoxicity profiles of networks based on DLD hybrids. Due to the high adhesion to soft tissue and the relatively fast degradability, the crosslinked material DLD-G4 × TEMPIC was chosen for the toxicity evaluation. A conventional eluting

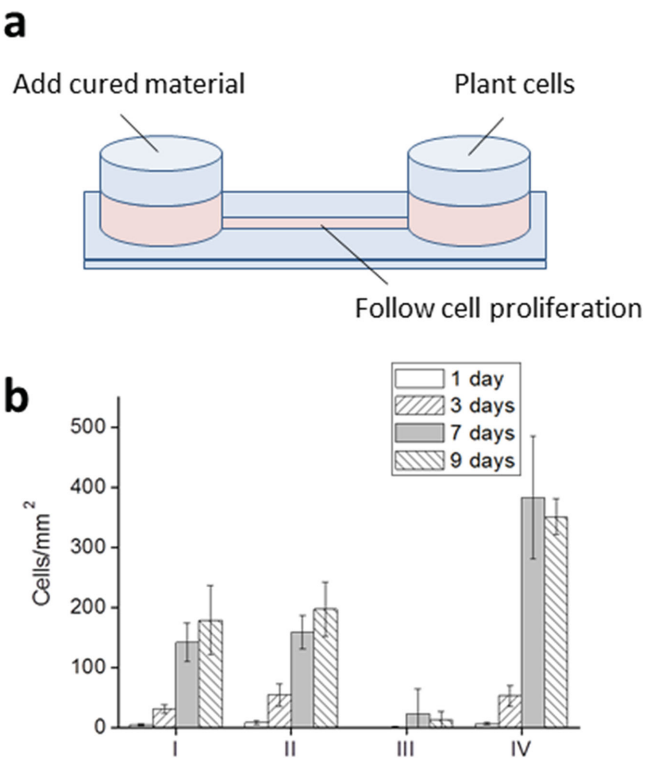

Figure 7. a) Schematic of test setup for observing cell proliferation over time. b) Proliferation of C3H/10T1/2 cells in the presence of I) DLD-G4 × TEMPIC (no CQ), II) DLD-G4 × TEMPIC (0.1 wt% CQ), III) Histoacryl, and IV) negative control.

method was used in order to investigate the survival of seeded human dermal fibroblast (hDF) cells in contact with material extracts. The results of the cytotoxicity test (**Figure 6**) present no leakage of cytotoxic concentrations of compounds from DLD-G4 × TEMPIC without the photoinitiator, camphorquinone (CQ). Similarly, networks containing 0.1 wt% CQ did not lead to an increased cytotoxicity. Visual comparison between the negative control and DLD-G4 × TEMPIC materials revealed similar cell density and adherent morphology. In contrast, the Histoacryl extract showed much higher cytotoxicity and the cell viability decreased to 40%. The hDF cells exposed to Histoacryl extracts show lower cell density, abnormal morphology, and less cell attachment on the tissue culture plate.

A novel method where Ibidi µ-Slides I based on two wells connected with a channel was used to observe the cell proliferation in the presence of the cured materials of Histoacryl and DLD-TEMPIC with and without CQ. Cured materials of 30 mg were placed in one well and C3H/10T1/2 cells were seeded in the other well (**Figure 7**a). The cells were allowed to proliferate and migrate through the channel for 9 d. An increased cell density with increased time can be detected (Figure 7b). No difference in cell morphology was observed, however, the cell growth was influenced by the type of the material tested. A stable increase in cell density is seen for the sample of DLD-G4 × TEMPIC with and without 0.1 wt% CQ as well as for the negative control. However, compared to the negative control, a lower final cell density after 9 d is displayed. The

DLD-G4 × TEMPIC conditions with and without CQ showed 57% and 51% of the cell density of the negative control, respectively. Histoacryl inhibited the cell proliferation more than the DLD-G4 × TEMPIC samples leading to a cell density of only 4% of the cell density of the negative control. Images of cells are presented in the Supporting Information (Figure S1, Supporting Information).

It should be noted that Histoacryl was difficult to cure into pieces of the desired dimensions. Thus, a larger surface area and cavities with unreacted resin may be contributing to the higher cytotoxicity.

Nonetheless, an advantage over Histoacryl can clearly be seen in the cytotoxicity studies of the DLD materials, where the combination of milder components and a more uniform curing leads to lower cytotoxicity. The combined properties of DLD-G4 × TEMPIC make the DLD STAP concept highly desired as biomedical adhesive.

The STAP technology, including the light induced fixation method, is well suited for novel methods of wound closures and repairs. The combination of the adhesive and the surgical mesh can implement a greater use of tissue adhesives and possibly replace unnecessary damaging fixation methods such as sutures and staples. Indeed, the high cost of fibrin sealants, the toxicity of cyanoacrylates, and the high swelling of conventional PEG-adhesives imply an unfulfilled need where the promising adhesives containing a DLD component can be a solution for tomorrow's biomedical adhesives.

3. Conclusions

In this study, a library of reactive DLD hybrids with low dispersities and applicable viscosities, originating from the highly branched structures, has successfully been synthesized and functionalized in large scale to be used as biomedical STAP components. Without the need of co-solvents, highly crosslinked networks with remarkably low swelling in comparison to conventional PEG-based adhesives were able to be formed together with TEMPIC through benign HEV-light initiated TEC. The variation of pseudo-generations of the dendritic structure is well reflected in the physical and mechanical properties of the materials over a range that is not covered by currently available tissue adhesives. The STAP of DLD-G4 × TEMPIC and a surgical mesh displayed a promising adhesive ability toward wet soft tissue and the adhesive showed no cytotoxicity of eluted extracts. The crosslinked materials displayed impaired mechanical properties after storage in HBP as well as PBS.

4. Experimental Section

Materials: PEG (BioUltra 2000 M_w = 2000 g mol^{-1}) (PEG), 4-(dimethylamino)pyridine (99%), 2-allyloxyethanol (98%), N,N′-dicyclohexylcarbodiimide (99%), chromium(III) acetylacetonate ($Cr(acac)_3$) (97%), CQ (97%), PBS (10× concentrate, BioReagent, suitable for cell culture, for molecular biology), and methanol (anhydrous, 99.8%) were purchased from Sigma-Aldrich. THIOCURE TEMPIC TEMPIC was generously provided by Bruno Bock. bis-MPA was kindly donated by Perstorp. Succinic anhydride and dichloromethane (analytical grade) were obtained from Merck. AnalR Normapur Pyridine was acquired from VWR. Chloroform-D ($CDCl_3$) (99.8%) and dimethyl sulfoxide-d6 (99.5%) (DMSO-d6) was obtained from Cil. Diethylether (analytical grade) (ether) was acquired from Fischer. 4-(2-(allyloxy) ethoxy)-4-oxobutanoic acid was prepared according to a previously published synthesis procedure.[29] Histoacryl was purchased from B. Braun. µ-slide I was purchased from Ibidi. PETKM2006 SurgicalMesh was purchased from Textile Development Associates, Inc. Mediskin Porcine Xenograft (unperforated) was kindly provided by Mölnlycke Health Care. All reagents for cell culturing in the extract cytotoxicity test were purchased from Thermo Scientific HyClone. AlamarBlue Assay, Basal Medium Eagle (BME) (GIBCO—Invitrogen), Gentamicin (GIBCO—Invitrogen), and L-Glutamine (GIBCO—Invitrogen) were purchased from Life Technologies. Fetal bovine serum (FBS) was obtained from Saveen Werner. HBP was kindly provided by Karolinska University Hospital.

Synthesis: A library of allyl-functionalized DLD hybrids was prepared according to a previously published procedure. The hyperbranched scaffolds were initially synthesized through bulk polycondensation reaction using sequential addition of bis-MPA to the chain ends of PEG.[12] The obtained DLDs, PEG-G*X*-OH, with pseudo-generations 3 to 6 (G3–G6) were then postfunctionalized with 4-(2-(allyloxy)ethoxy)-4-oxobutanoic anhydride (allyloxy anhydride) to form PEG-G*X*-Allyl (DLD-G*X*). Descriptions of the DLD-G*X* syntheses are given in the Supporting Information.

Methods for Component Analysis: FT-IR spectroscopy was executed using a Perkin-Elmer Spectrum 2000 FT-IR instrument equipped with a heat controlled single reflection attenuated total reflection (ATR) accessory (Golden Gate heat controlled) from Specac Ltd. Wavenumbers of 600–4000 cm^{-1} and a resolution of 4 cm^{-1} were used. Background normalization was performed with an average from 16 scans. Each sample was analyzed with 16 scans. The spectra were normalized using the peak of $-CH_2-$ from the PEG core (1465 cm^{-1}). The presence of carbonyl shift (1730 cm^{-1}) and the absence of carboxyl shift (1685 cm^{-1}) were used to confirm the conversion of bis-MPA to hyperbranched structures.

FT-Raman spectroscopy was conducted on a Perkin-Elmer Spectrum 2000 NIR FT-Raman instrument. Each sample was analyzed through 32 scans with a laser power of 500 mW. The spectra were normalized using the carbonyl shift (1765 cm^{-1}). The shifts of thiol groups (2575 cm^{-1}) and allyl groups (1645 cm^{-1}) were analyzed to confirm the TEC reaction.

NMR spectroscopy was performed using a Bruker AM NMR and the spectra were analyzed with MestReNova version 7.1.2-10008 (Mestrelab Research S.L. 2012). ^{1}H-NMR was recorded at 400 MHz using 628 scans on a solution of 10–20 mg mL^{-1} of the analyzed material dissolved in $CDCl_3$. ^{13}C-NMR was recorded at 100 MHz using 2048 scans on a solution of 150 mg mL^{-1} of the analyzed material dissolved in $CDCl_3$. Quantitative ^{13}C-NMR were acquired with an inverse gated decoupling method using 2048 scans and a relaxation time of 5 s on a solution of 15 mg $Cr(acac)_3$ and 150 mg of the analyzed material in 1 mL DMSO-d6.

DB of the DLDs was calculated using the Frechet equation,[24] (Equation (1)). The number of terminal (T), linear (L), and dendritic (D) groups of the hyperbranched bis-MPA structure was analyzed according to earlier presented work on bis-MPA[25]

$$\left(\text{Degree of branching} = \frac{D+T}{D+T+L}\right) \quad (1)$$

DSC was executed with a Mettler Toledo DSC820. The measurements were performed using a temperature cycle program to heat the sample from 25 to 80 °C, followed by cooling the sample down to –80 °C and finally heat the sample to 80 °C. Temperature adjustment with a rate of 5 °C min^{-1} was used and the temperature was kept constant for 2 min at 80 °C and –80 °C. Characterizations were made on the second heating period with STARe Software.

SEC was performed on a TOSOH EcoSEC HLC-8320GPC equipped with an EcoSEC RI detector and three columns (PSS PFG 5 µm; Microguard, 100 and 300Å) (M_W resolving range 100–300 000 g mol^{-1}) from PSS GmbH. The mobile phase used was dimethylformamide

(0.2 mL min^{-1}) with 0.01 M LiBr at a temperature of 50 °C. Samples with a concentration of 2 mg mL^{-1} were used and the results were calibrated with a conventional method using linear PEG standards. Analyses were made using PSS WinGPC Unity software version 7.2.

Rheometry was performed using a Discovery Hybrid Rheometer II from TA Instruments with a complete Peltier Plate Temperature System and a 20 mm parallel plate at a temperature of 35 °C with a geometry gap of 100 μm and 1 min of conditioning before start. Analyses were made from shear rates of 0.02–200 s^{-1}.

Preparation of Chemically Crosslinked Materials: Resins constituting of one of the DLD compounds and TEMPIC (DLD-G*X* × TEMPIC) were prepared to contain equal amounts of allyl and thiol groups. CQ (0.1 wt%) was added as photoinitiator. Crosslinked dumbbells and discs were molded in Teflon molds. Curing of the materials via TEC chemistry was induced with a light emitting diode polymerization lamp (Bluephase 20i) intended for light-cured dental materials. Bluephase 20i emits light with wavelengths of 385–515 nm with a dominant wavelength of 470 nm and maximum intensity of 2000–2200 mW cm^{-2}. If not stated otherwise, the curing was performed with the high power program (1200 mW cm^{-2}) using a total irradiation time of 30 s per area unit at a distance of under 1 mm between sample and light source. The samples were allowed to postcure for 1 d after irradiation. The dimensions of the middle section of the dumbbells were 9 × 3 × 1 mm. The discs for swelling and degradation studies had a diameter of 4 mm and a thickness of 2 mm.

Evaluation of Crosslinked Materials: Swelling studies were executed by keeping the crosslinked materials submerged in PBS (pH = 7.4, phosphate buffer 0.01 M, NaCl 0.154 M) in an oven at 37 °C. The weight of the materials before submersion (m_{dry}) was obtained after drying the materials in a vacuum oven at 50 °C for 2 h. The weight of the swollen materials ($m_{swollen}$) was obtained after having the materials submerged for 10 min, 30 min, 90 min, 1 d, 1 week, and 1 month and the degree of swelling was calculated (Equation (2)). Triplicates of each sample were used

$$\left(\text{Degree of swelling} = \frac{m_{swollen} - m_{dry}}{m_{dry}}\right) \quad (2)$$

Gel fractions were acquired by comparing the dry weight of crosslinked materials before and after being leached in chloroform for 5 h at room temperature under gentle shaking. The chloroform was exchanged after 20 min, 1 and 3 h. The process was monitored with ^{1}H-NMR using $CDCl_3$ as solvent to confirm fully leached materials. The materials were dried in a vacuum oven at 50 °C for 24 h prior to weighing the leached material ($m_{leached}$) and the GFs were calculated (Equation (3)). Triplicates of each material were used

$$\left(\text{Gel fraction} = \frac{m_{leached}}{m_{start}}\right) \quad (3)$$

The condition of the crosslinked materials after being exposed to simulated physiological environment was studied both by weight loss and by examining the mechanical properties. One setup of the materials was submerged in PBS (pH 7.4, phosphate buffer 0.01 M, NaCl 0.154 M) and kept at 37 °C. The materials were tested dry and after being submerged for 1 d, 1 week, and 1 month. Another setup of materials was submerged in HBP and stored at 37 °C for 1 week, 1 month, and 3 months prior to testing. Tensile tests were performed using an Instron 5944 from Instron Korea LLC, using a 500N load cell and a cross-head speed of 10 mm min^{-1}. A preload of 1 N and a preload speed of 5 mm min^{-1} were used. The measurements were conducted at 23 °C and a relative humidity of 50%. All samples were acclimatized to the testing environment. Samples in the wet state were kept wet as long as possible until they were attached to the Instron. Data were collected using Bluehill software. Young's modulus (E) was calculated from the initial linear region of the stress (σ) and strain (ε) curve. Triplicates or quadruplicates of each material and condition were used.

Weight loss was calculated by comparing the dry weight of the materials before (m_{start}) and after the treatment ($m_{deg.}$) (Equation (4)). The m_{start} was obtained after drying the samples in a vacuum oven for 2 h at 50 °C. The $m_{deg.}$ was obtained after removing the samples from the storage conditions, washing with deionized water and dry in vacuum oven for 24 h at 50 °C. Triplicates of each sample were used

$$\left(\text{Weight loss} = \frac{m_{start} - m_{deg.}}{m_{start}}\right) \quad (4)$$

Adhesion of Biomedical Adhesive to Soft Tissue: Porcine skin substrates were prepared by thawing and cutting Mediskin Porcine Xenograft (unperforated) into 4 × 2.5 cm dimensions, which subsequently were glued onto test fixtures of 6 × 4 × 0.15 cm sized poly(methyl methacrylate) PMMA pieces with Super Glue Brush on Loctite. The substrates were kept submerged in PBS (pH 7.4, phosphate buffer 0.01 M, NaCl 0.145 M) bath at 37 °C until the tested resins were applied. The substrates were removed from the bath and excess water was wiped off with nonwoven swabs (Selefa). Surgical mesh pieces of 2 × 2.5 cm were placed to bridge together the substrates in pairs. Resin was applied to bind the surgical mesh to the porcine skin over an area of 1 × 2.5 cm per substrate. Curing was induced with Bluephase 20i HIGH POWER program for 2 min per substrate pair for the light-cured resins. The glued samples were returned to the PBS bath for conditioning for 1 h at 37 °C. The submerged samples were allowed to reach 23 °C in order to acclimatize the samples to testing environment. Adhesive bond shear strength was tested using an Instron 5944 from Instron Korea LLC, using a 500N load cell and a cross-head speed of 5 mm min^{-1} in tensile mode. A preload of 0.5 N and a preload speed of 2 mm min^{-1} were used. The measurements were conducted at 23 °C and a relative humidity of 50%. The samples were kept wet until they were attached to the machine. Data were collected using Bluehill software. Adhesive bond shear strength was calculated from maximum load at break divided by the area of failure. Quadruplicates of each sample were used.

Cytotoxicity: In vitro cytotoxicity studies were conducted on DLD-G4 × TEMPIC networks cured with and without CQ photoinitiator using Bluephase 20i and compared to Histoacryl tissue adhesive. Histoacryl was left to cure for 24 h before testing. In one study, hDFs were employed to investigate the leaching of potential toxins from the materials. The hDF cells were cultured in complete growth medium (CGM). CGM is Dulbecco's Modified Eagles Medium (DMEM-F12 medium) supplemented with 10% FBS, penicillin (100 U mL^{-1}), and streptomycin (100 μg mL^{-1}). The culture was kept in an incubator at 37 °C and 5% CO in a humidified atmosphere. Cells were harvested using trypsin-EDTA and the cell density was evaluated with aid of hemocytometer. The eluting tests were performed according to ISO10993-5 procedures. All materials were rinsed in 70% ethanol for sterilization and then washed for three times with sterile PBS. The materials were leached in CGM in a tissue culture plate for 24 h at 37 °C and 5% CO with a weight/volume ratio of 0.2 g mL^{-1}. Then 0.5 mL extract medium was added to each well in a 48-well tissue culture plate and 5 × 10^4 hDF cells were seeded to each well with extract medium. Cells were cultured for 24 h in an incubator at 37 °C and 5% CO in a humidified atmosphere. The negative control was the CGM extract of an empty well in the tissue culture plate. The positive control included 5% DMSO in CGM. Samples were run in triplicate. The metabolic activity of hDF cells were evaluated with alamarBlue Assay (Life Technology) according to the instruction from the manufacturer. The fluorescent intensity indicating the viability of the cells was measured with a plate reader (Tecan Infinite M200 Pro) with excitation at 560 nm and emission at 590 nm. Cells cultured in extract medium were observed under light microscopy (Nikon Eclipse TE2000-U) to evaluate the cell density and morphology.

In the second study, the proliferation of a mouse embryonic fibroblast cell line, C3H/10T1/2 (ATCC-CCL-226 LGC standards), was evaluated in the presence of DLD-G4 × TEMPIC networks. Cells were cultured using BME (GIBCO—Invitrogen), containing 10% FBS (Saveen Werner), 1% Gentamicin (GIBCO—Invitrogen), and 1% L-Glutamine (GIBCO—Invitrogen), in an incubator with 5% CO_2. The cytotoxicity of the materials was evaluated in triplicates by C3H/10T1/2 cell proliferation using Ibidi μ-Slides I (Ibidi). About 1000 cells were plated in one well of each slide and 30 mg of the tested material in the other well. Cell

proliferation was observed along the slide channel over 9 d and images were taken during this time at days 1, 3, 7, and 9. Cells were observed under light microscopy (Olympus CKX41 equipped with Olympus SP510UZ camera) to quantify the cell density and evaluate the cell morphology.

Supporting Information

Supporting Information is available from the Wiley Online Library or from the author.

Acknowledgements

The authors acknowledge Knut och Alice Wallenbergs Stiftelse for financial support and Mölnlycke Health Care AB for the provision of Mediskin Porcine Xenograft.

Received: August 3, 2015
Revised: September 2, 2015
Published online: September 30, 2015

[1] a) T. E. MacGillivray, *J. Card. Surg.* **2003**, *18*, 480; b) A. Rajimwale, B. K. Golden, S. Oottomasathien, M. Krishnamurthy, N. O. Ullrich, M. A. Koyle, *J. Urology* **2004**, *171*, 2407; c) M. H. Osmond, T. P. Klassen, J. V. Quinn, *J. Pediatr.* **1995**, *126*, 892.

[2] a) D. H. Sierra, K. O'Grady, D. M. Toriumi, P. A. Foresman, G. T. Rodeheaver, A. Eberhardt, D. S. Feldman, J. E. Lemons, *J. Biomed. Mater. Res.* **2000**, *52*, 534; b) J. M. G. Paez, E. J. Herrero, A. Rocha, M. Maestro, J. L. Castillo-Olivares, *J. Mater. Sci.: Mater. Med.* **2004**, *15*, 109; c) A. N. Azadani, P. B. Matthews, L. Ge, Y. Shen, C. S. Jhun, T. S. Guy, E. E. Tseng, *Ann. Thorac. Surg.* **2009**, *87*, 1154.

[3] G. Schneider, K. Otto, *Arch. Oto-Rhino-Laryngol.* **2012**, *269*, 1783.

[4] a) R. Marcovich, A. L. Williams, M. A. Rubin, J. S. Wolf, *Urology* **2001**, *57*, 806; b) A. Ekelund, O. S. Nilsson, *Int. Orthop.* **1991**, *15*, 331.

[5] G. Ciapetti, S. Stea, E. Cenni, A. Sudanese, D. Marraro, A. Toni, A. Pizzoferrato, *Biomaterials* **1994**, *15*, 63.

[6] L. P. Bre, Y. Zheng, A. P. Pego, W. Wang, *Biomater. Sci.* **2013**, *1*, 239.

[7] a) C. R. Berney, A. E. T. Yeo, *Hernia* **2013**, *17*, 709; b) B. Novik, S. Hagedorn, U. B. Mork, K. Dahlin, S. Skullman, J. Dalenback, *Surg. Endosc.* **2006**, *20*, 462; c) P. Topart, F. Vandenbroucke, P. Lozac'h, *Surg. Endosc.* **2005**, *19*, 724.

[8] a) H. B. Zhang, A. Patel, A. K. Gaharwar, S. M. Mihaila, G. Iviglia, S. Mukundan, H. Bae, H. Yang, A. Khademhosseini, *Biomacromolecules* **2013**, *14*, 1299; b) M. H. M. Oudshoorn, R. Rissmann, J. A. Bouwstra, W. E. Hennink, *Biomaterials* **2006**, *27*, 5471; c) H. Altin, I. Kosif, R. Sanyal, *Macromolecules* **2010**, *43*, 3801.

[9] A. J. Velazquez, M. A. Carnahan, J. Kristinsson, S. Stinnett, M. W. Grinstaff, T. Kim, *Arch. Ophthalmol. (Chicago, IL, USA)* **2004**, *122*, 867.

[10] A. M. Oelker, J. A. Berlin, M. Wathier, M. W. Grinstaff, *Biomacromolecules* **2011**, *12*, 1658.

[11] D. Holter, A. Burgath, H. Frey, *Acta Polym.* **1997**, *48*, 30.

[12] O. C. J. Andrén, M. V. Walter, T. Yang, A. Hult, M. Malkoch, *Macromolecules* **2013**, *46*, 3726.

[13] H. Zhang, L. P. Bré, T. Zhao, Y. Zheng, B. Newland, W. Wang, *Biomaterials* **2014**, *35*, 711.

[14] H. Zhang, L. Bre, T. Y. Zhao, B. Newland, M. Da Costa, W. X. Wang, *J. Mater. Chem. B.* **2014**, *2*, 4067.

[15] a) A. Hult, M. Johansson, E. Malmstrom, *Adv. Polym. Sci.* **1999**, *143*, 1; b) Y. H. Kim, O. W. Webster, *Macromolecules* **1992**, *25*, 5561.

[16] H. Claesson, E. Malmstrom, M. Johansson, A. Hult, *Polymer* **2002**, *43*, 3511.

[17] a) C. E. Hoyle, C. N. Bowman, *Angew. Chem. Int. Ed.* **2010**, *49*, 1540; b) C. E. Hoyle, T. Y. Lee, T. Roper, *J. Polym. Sci., Part A: Polym. Chem.* **2004**, *42*, 5301.

[18] Q. Fu, J. H. Liu, W. F. Shi, *Prog. Org. Coat.* **2008**, *63*, 100.

[19] a) A. Nordberg, H. von Holst, K. Brolin, A. Beckman, *Biomed. Mater. Eng.* **2007**, *17*, 299; b) K. Pedersen, A. Nordberg, P. Halldin, H. von Holst, *J. Trauma Treat.* **2014**. *S2*, 007.

[20] H. A. Kayaoglu, O. F. Ersoy, N. Ozkan, A. Celik, N. O. Filiz, *Kaohsiung J. Med. Sci.* **2009**, *25*, 177.

[21] a) K. Oberg, Y. Hed, I. J. Rahmn, J. Kelly, P. Lowenhielm, M. Malkoch, *Chem. Commun.* **2013**, *49*, 6938; b) Y. Hed, K. Oberg, S. Berg, A. Nordberg, H. von Holst, M. Malkoch, *J. Mater. Chem. B* **2013**, *1*, 6015.

[22] a) B. D. Ratner, A. S. Hoffman, F. J. Schoen, J. E. Lemons, *Biomaterials Science – An Introduction to Materials in Medicine*, 2nd ed., Elsevier, San Diego, CA, USA/ London, UK **2004**, p. 573; b) N. Feliu, M. V. Walter, M. I. Montanez, A. Kunzmann, A. Hult, A. Nystrom, M. Malkoch, B. Fadeel, *Biomaterials* **2012**, *33*, 1970; c) R. Reul, T. Renette, N. Bege, T. Kissel, *Int. J. Pharm.* **2011**, *407*, 190.

[23] A. Nordberg, P. Antoni, M. I. Montanez, A. Hult, H. Von Holst, M. Malkoch, *ACS Appl. Mater. Interfaces* **2010**, *2*, 654.

[24] C. J. Hawker, R. Lee, J. M. J. Frechet, *J. Am. Chem. Soc.* **1991**, *113*, 4583.

[25] H. Magnusson, E. Malmstrom, A. Hult, *Macromolecules* **2000**, *33*, 3099.

[26] a) I. Sendijarevic, A. J. McHugh, *Macromolecules* **2000**, *33*, 590; b) P. J. Farrington, C. J. Hawker, J. M. J. Frechet, M. E. Mackay, *Macromolecules* **1998**, *31*, 5043.

[27] a) P. K. Campbell, S. L. Bennett, A. Driscoll, A. S. Sawhney, *Evaluation of Absorbable Surgical Sealants: In vitro Testing*, Confluent Surgical, Inc., Waltham, MA, USA, **2005**; b) M. Mehdizadeh, H. Weng, D. Gyawali, L. P. Tang, J. Yang, *Biomaterials* **2012**, *33*, 7972.

[28] D. G. Barrett, G. G. Bushnell, P. B. Messersmith, *Adv. Healthcare Mater.* **2013**, *2*, 745.

[29] P. Lundberg, A. Bruin, J. W. Klijnstra, A. M. Nystrom, M. Johansson, M. Malkoch, A. Hult, *ACS Appl. Mater. Interfaces* **2010**, *2*, 903.